Biogeosciences Discuss., 6, 5373–5408, 2009
www.biogeosciences-discuss.net/6/5373/2009/

Biogeosciences
Discussions

Biogeosciences Discussions is the access reviewed discussion forum of *Biogeosciences*

Benthic phosphorus and iron budgets for NW-African slope sediments; biogeochemical processes and the importance of bioturbation

K. Küster-Heins[1], **G. J. de Lange**[2], **and M. Zabel**[3]

[1] Department of Geosciences, Univ. of Bremen, Klagenfurter Str., 28359 Bremen, Germany
[2] Department of Earth Sciences – Geochemistry, Faculty of Geosciences, Utrecht Univ., 3508 TA Utrecht, The Netherlands
[3] Marum – Center for Marine Environmental Sciences, Univ. of Bremen, Leobener Str., 28359 Bremen, Germany

Received: 13 May 2009 – Accepted: 20 May 2009 – Published: 29 May 2009

Correspondence to: K. Küster-Heins (snoepje@uni-bremen.de)

Published by Copernicus Publications on behalf of the European Geosciences Union.

Abstract

Despite intensive research on the different domains of the marine phosphorus (P) cycle during the last decades, frequently discussed open questions still exist especially on controlling factors for the benthic behaviour of P and its general distribution in sediment-pore water systems. Steady state or the internal balance of all relevant physical and (bio)geochemical processes are amongst the key issues. In this study we present and discuss an extended data set from surface sediments recovered from three locations on the NW-African continental slope. Pore water data and results from sequential sediment extractions indicate a close relationship between the benthic cycles of P and iron. Accordingly, most of the dissolved phosphate must have been recently released by microbially catalyzed reductive dissolution of iron (oxhydr)oxides. However, rates of release and association of P and iron, respectively, are not directly represented in profiles of element specific sediment compositions. Steady-state based transport-reaction modelling results suggest that particle mixing due to active bioturbation, or rather a physical net downward transport of P associated to iron (oxyhydr)oxides, is an essential process for the balance of the inspected benthic cycles. This study emphasizes the importance of balancing analytical data so as to provide for a more comprehensive interpretation of all relevant processes.

1 Introduction

Marine sediments are the largest reservoirs of phosphorus on Earth (e.g. Van Cappellen and Ingall, 1994). In particular, continental shelf and upper slope sediments are important sinks for major biogeochemical elements, like carbon, nitrogen, or just P. These regions are generally characterized by a large input of organic material through vertical settling from the euphotic zone and lateral transport (e.g. Jahnke et al., 1989; Kim et al., 1999; Inthorn et al., 2006). For the most part, the particulate organic material is already decomposed during its pathway through the water column. However, a minor but important portion arrives at the sea floor where microbial degradation processes continue and lead to the release of dissolved phosphate into bottom and interstitial waters. Following the burial pathway, the sequence of early diagenetic reactions seems to dominate the benthic P cycle and therefore the distribution of P in marine sediments. Here a variety of environmental conditions, geochemical and biogeochemical processes determine how much phosphorus is released back to the oceans nutrient cycle or buried for geological periods of time.

During the last decades, the number of studies looking on different, specific parts of the benthic P-cycle has multiplied. Such studies ranged from regional to global distribution of phosphatic sediments and rocks (e.g. Baturin, 1982; Föllmi, 1996), to investigations on the recent formation of phosphorites (e.g. Froelich et al., 1988; Schenau et al., 2000; Schulz and Schulz, 2005), from detailed inspections of the benthic P-cycle on local and regional scales (e.g. Sundby et al., 1992; Ingall and Jahnke, 1994; Anschutz et al., 1998) to basin-wide quantifications of the benthic phosphate release (Zabel et al., 1998; Hensen et al., 1998), from the identification and quantification of phosphorus forms in marine sediments (e.g. De Lange, 1992; Ruttenberg, 1992; Schenau and De Lange, 2000) to steady-state modelling of the sediment-pore water system with special focus on the behaviour of phosphorus (e.g. Slomp et al., 1996, 1998). These studies have resulted in an improved understanding of P-cycling in marine sediments. However, nearly all of them have focused on specific subdomains without taking the total balance of the benthic system into account. Certainly, for example Sundby et al. (1992) have derived a general scheme of the interrelating processes of the benthic P fluxes, but release and precipitation rates have not been used to balance corresponding mass transfers. In this regard, the combination of analytical results with steady-state transport-reaction modelling, which have been carried out by Slomp et al. (1996, 1998), can be seen as the most complete one. However, focusing on the authigenic formation of apatite and the role of P adsorption in shallow water sediment, respectively, the importance of bioturbation for the balance of the benthic P-cycle has been discussed only marginally. For this study, we investigated the phosphorus geochemistry at three sites on the continental margin of NW-Africa. An extensive data set with varying analyses of pore waters and sediments was generated for the purposes (1) to unravel the local geochemical conditions that control the benthic P- and Fe-cycles, and (2) to identify, understand and quantify the processes that affect the (re)distribution of P in surface sediments.

2 Material and methods

2.1 Study area and sampling sites

We present results from sediment investigations on three cores, recovered during RV Meteor cruise leg M65/1 along the northwestern African continental margin (Mulitza et al., 2006; Fig. 1, Table 1). In this region, seasonal variations of northeast trade wind position and intensity control the westward directed transport of near-shore surface waters (Canary Current; e.g. Mittelstaedt, 1983; Helmke et al., 2005). The Canary Current, a broad eastern boundary current, flows from Morocco southward toward the Cape Verde Islands, where it joins the westward flowing North Equatorial Under Current and primary South Atlantic Central Water (McMaster and Lachance, 1969; Helmke et al., 2005). The South Atlantic Central Water is the main source of nutrient-rich water masses, leading to a 50–70 km wide coastal band of intensive upwelling (Hagen, 1981, 2000; Lutze and Coulbourn, 1984; Helmke et al., 2005). The northern-most site GeoB 9510 is located between the Senegal River and Dakar, where terrigenous silty-clayey muds dominate (Barusseau et al., 1988; Mulitza et al., 2006). GeoB sites 9519 and 9518 are located slightly south between Dakar and the Gambia River. Here terrigenous sandy muds are abundant along the coast. Off Senegal, relatively low carbonate contents of 8.1 to 13.5 wt% (Table 1) are indicative of the dominance of land-derived material in these sediments (e.g. McMaster and Lachance, 1969; Hartmann et al., 1976). According to Summerhayes (1983), the relatively low contents of organic carbon in the studied surface sediments (2.4–2.9 wt%; Table 1) are the result of intensive turbulence and turbidity, which favour intense recycling of biogenic compounds already in the water column. Besides, in a recent study by Mollenhauer et al. (2007) significant differences in radiocarbon contents are observed in sediments off NW-Africa. Accumulated organic material is older than the vertically settled original biogenic debris, caused by resuspension in the water column by lateral transport processes across the shelf.

2.2 Sediment and pore water sampling

Sediment cores were taken with a multicorer and processed under situ temperature (4°C) directly upon retrieval. Overlying bottom waters were sampled and filtered for subsequent measurements. Two different extraction methods have been used for porewaters of this study: squezzing and rhizon sampling. At all sites Teflon pore water squeezers were used (Schulz et al., 1994; Zabel et al., 1998), subsequently operated in a glovebox with argon at a pressure gradually increasing up to 5 bar. The pore water was retrieved through 0.2 μm cellulose acetate filters. In addition, at sites GeoB 9518 and 9519, rhizon samplers (~0.4 μm) were used (Seeberg-Elverfeldt et al., 2005; Dickens et al., 2007). No significant differences were detected between both pore water extraction methods for NO_3^-, NH_4^+ and alkalinity concentrations. However, for ferrous iron and phosphate much higher levels occurred when retrieved with rhizons (GeoB 9518 and 9519). This can be attributed to the high sensitivity of ferrous iron to even very low oxygen concentrations such as may have occurred during the squezzers porewater extraction process (e.g. De Lange et al., 1992). The phosphate concentrations are affected as well, due to the strong affinity of phoshate to adsorb on iron (oxyhydr)oxide. We will use rhizon porewater data for further calculations, but indicate the squezzer data for comparison (Fig. 2).

Solid phase samples for total digestions and sequential extraction analysis were sectioned at 0.5–5 cm intervals and stored at −20°C.

2.3 Pore water analysis and flux calculations

Pore water analyses were carried out on board within a few hours after pore water sampling: ammonium, phosphate, ferrous iron and nitrate. A detailed description of the used standard methods is given in Table 2. Aliquots of the remaining pore water samples were diluted 1:10 with demineralized water and acidified with 1% $HNO_{3\ (suprapure)}$ and stored at 4°C. Diluted squezzer samples were used for subsequent analyses of manganese and total sulphur at the University of Bremen using an inductively coupled plasma atomic emission spectrometer (ICP-OES, Perkin Elmer Optima 3000).

The diffusive transport rates of dissolved phosphate and iron were determined by applying Fick's First Law of diffusion: molecular flux $(J)=-\varphi\times D_0\times(1-\ln(\varphi^2))^{-1}\times\partial C/\partial x$ (Schulz, 2006). The porosity (φ) is assumed to be constant at 0.8, the temperature- and substance-dependent diffusion coefficient ($D_0 4°C$) is 123 $cm^2 a^{-1}$ and 124 $cm^2 a^{-1}$ for phosphate and ferrous iron, and $\partial C/\partial x$ reflects the specific concentration gradient. For modelling of pore water concentration profiles, the computer model Explicite was used (Zabel and Schulz, 2001; Schulz and Schulz, 2005; Schulz, 2006). Balancing of the systems base on the simplification of a constant wet bulk density of 0.4 g cm^{-3}.

2.4 Solid phase analysis

Bulk concentrations of major elements in sediments were determined after total digestion in a HNO_3 (65%), HCl (30%) and HF (47–51%) mixture using a Microwave system (Zabel et al., 1999). Dissolved elemental concentrations of P, iron (Fe), calcium (Ca) and sulphur (S) were measured with ICP-OES.

The solid-phase speciation of P in the sediments from GeoB 9510 and 9519 was examined using a five-step sequential extraction scheme, where approximately 0.125 g of dried and ground sediment sample was washed with 25 mL (1) 2 M NH_4Cl (pH 7; step repeated ten times), (2) citrate dithionite buffer (CDB; pH 7.5), (3) 1 M sodium acetate buffer (pH 4), (4) 1 M HCl, and (5) 1 M HCl after ignition at 550°C. After step (2) and (3) samples were rinsed successively with 25 mL 2 M NH_4Cl and 25 mL demineralized water to prevent the readsorption of phosphate. This extraction analysis is after Ruttenberg (1992) and Schenau and De Lange (2000) (Table 3). Comparing the sum of extracted P and the separately determined total-P content of the sediment, good to fair correspondence was obtained for cores 9510 and 9519, whereas there was a substantial difference for core 9518. Therefore, residues for the latter sediments were additionally extracted with (6) 25 mL 1.5 M sodium hydroxide solution at 85°C, to determine the opal-associated phosphate fraction according to Latimer et al. (2006) (Table 3). Despite of the recovery of a significant fraction of opal-associated P, most of the discrepancy remained for this core. The concentration of P released to each leaching solution was quantified automatically with a Skalar Autoanalyser (SA 6250) at 880 nm, except P and Fe concentration in the CDB solutions and opal-associated P, which were determined with ICP-OES. For all ICP-OES measurements, application of standard reference material (USGS standard MAG-1, in-house standard MAX) assured the accuracy, as their element concentration were within certified range. The precision of analyses was <5%.

Total organic carbon (TOC) and total carbon (C_{tot}) were analysed on dried and ground samples with a Leco CS 200. This was done by analysing the untreated and decarbonated (using 12.5% HCl) samples, $\%CaCO_3$ being the difference between these two, was calculated as: $CaCO_3\%=(C_{tot}-TOC)\times 8.33$. Several standards with C contents of 0.8–12% were applied to maintain accuracy within a range of 1%.

For each core sub-samples from 0–0.5, 4–5, 7.5–10, 15–20 cm sediment depth were used for radiocarbon dating of TOC following standard procedures (Leibniz-Labor AMS facility at the Christian-Albrechts University Kiel, Germany; Nadeau et al., 1997).

3 Results

3.1 Pore water geochemistry

Pore water results reflect the distribution of major diagenetic compounds expected during the general early oxidation sequence of organic matter in the upper sediment column (Fig. 2). The nitrate concentration increases from the bottom water value (22.6–25.6 μmol L^{-1}) to a maximum (30.1–39.1 μmol L^{-1}) close to the sediment water interface. Dissolved manganese concentrations are low at the sediment surface (<0.2 μmol L^{-1}), but at the depth between nitrate maximum and nitrate depletion, they start to increase towards a concentration of 6.1–8.1 μmol L^{-1} at depth. Ammonium and alkalinity show the normal gradual increase with increasing sediment depth. However, small changes in the gradients of the ammonium profiles can be observed at depths around 6 cm. Total sulphur, or rather sulphate concentrations (no sulphide could be detected) keeps almost constant throughout the core lengths. All three cores show pronounced peaks in ferrous iron and phosphate pore water concentrations at a depth of 3 and 7 cm. All phosphate profiles show two, more or less distinct local maxima. The upper one was detected when nitrate is nearly exhausted; the lower parallels the iron peak.

3.2 Sediment composition

In all three sedimentary settings, profiles of bulk P exhibit local maxima of 0.82–0.96 g kg^{-1} around 2 cm sediment depths (Fig. 3). Below these enrichments, data reveal decreases of about 14–22%. According to the results of the sequential extraction procedure, 0.62–0.87 g P kg^{-1} could be assigned to specific carrier phases, which corresponds to a recovery of 84–100% of the total P content in these sediments (Fig. 3). The fractions of oxide-associated P, NH_4Cl-extractable biogenic P, and organic-bound P (steps 1, 2 and 5) are nearly equivalent (Table 4). However the ratios between these three pools change with sediment depth. While the proportion of biogenic P (step 1) remains relatively constant, the oxide-associated fraction (step 2) and the organic-bound P (step 5) seem to be negatively correlated, with significant higher values for the oxide fraction close to the sediment surface. Compared with the main fractions, the detrital, the opal-associated, and authigenic apatite fractions are negligible (5–11%, 11%, and 5–7% of total P, respectively; Table 4). Only subtle differences appear to occur for the dominant P-carrying phases between the three cores.

Sequential leaching with NH_4Cl and subsequent measurement of Ca and P give information on the presence of biogenic apatite (e.g. fish debris) and/or $CaCO_3$-phosphates. Biogenic apatite is soluble with NH_4Cl extraction once all soluble Ca has been extracted. Therefore, at least ten successive extractions with NH_4Cl are usually required to determine in which NH_4Cl step the biogenic apatite fraction is extracted (Schenau and De Lange, 2000; Fig. 4). Highest concentrations of Ca and P were measured after the first extractions with NH_4Cl, probably associated with exchangeable P and P associated with carbonates.

The total sedimentary Fe concentrations (Fe_{tot}) are in the range of 33.3–40.0 g kg^{-1} (Fig. 5). Apart from a general increase by 3–16% between the surface layer and the core bottom, prominent local maxima exist at about 1.5–2.0 cm sediment depth. These characteristic features are mainly caused by iron (oxyhydr)oxides (Fe_{CDB}, step 2) which come from up here to a maximum of 8 g kg^{-1} or 23% of the total Fe content. Below this enrichment layer the Fe_{CDB} fractions decrease by 21–29% within narrow depth intervals of 2 cm only. The total decrease of CDB extractable Fe fraction with increasing sediment depth amounts to 42–50%, an observation which has already been documented for continental margin sediments (Anschutz et al., 1998). However, the local maxima in the upper sediment column are parallel to the distribution of P_{CDB} (Fig. 5).

Total organic carbon (TOC) and total carbonate contents remain relatively constant in all three cores (Fig. 6). However, maxima in TOC occur at the sediment surface (1.8 to 3.2 wt%), and the carbonate content increases slightly with depth (max. 10.1 to 15.2 wt%). The molar C_{org}:P_{org} ratios are generally high with values of up to 500 for instance at site GeoB 9518.

Title Page
Abstract | Introduction
Conclusions | References
Tables | Figures
◀| |▶
◀ ▶
Back | Close
Full Screen / Esc
Printer-friendly Version
Interactive Discussion

Radiocarbon dating of total organic carbon reveals that all dated sediment constituents are of Holocene age (^{14}C ages < 3200 yr BP, Table 5). Data deviate from a normal linear increase in age with increasing sediment depth. We interpret this to be related to bioturbative processes, since visual core description did not indicate slumping (R. Tjallingii, personal communication). Regardless of some scatter, these data reveal more or less continuous sedimentation, which allows the calculation of approximate average sedimentation rates (6.3–8.6 cm kyr^{-1}). Using approximate sedimentation rates would not significantly change modelling results and subsequent conclusions.

4 Discussion

4.1 The benthic P- and Fe-cycle – sources and sinks

The first downward increase of pore water phosphate under oxic conditions is attributed to microbially mediated organic matter mineralization (e.g. Froelich et al., 1979; Jahnke et al., 1989). The total release of P by this process is hard to quantify. Generally, the consumption of major electron acceptors like oxygen or nitrate cannot be attributed to the microbial oxidation of organic substance exclusively. Reoxidation of reduced species has to be taken into consideration, although this may be of less quantitative importance in most environments. A probably more significant uncertainty exists on the composition of the organic matter itself or rather of the portion which is degraded. It is striking that our C_{org}:P_{org} ratios of 300–400 for the three cores (Fig. 6) are far beyond the primary composition of the organic matter generally produced in the C (106–140:1; Redfield et al., 1963; Takahashi et al., 1985). These findings correspond to those from other studies (e.g. Ingall and Van Cappellen, 1990; Anderson et al., 2001). Accordingly, such high ratios may document enhanced regeneration and removal of labile particulate P relative to organic carbon. The remains, which are preserved in the sediments after preferential P (and N) depletion, are a relatively refractory organic component. However, despite the observed impoverishment of the organic substance, our pore water data let indicate a permanent, net phosphate release from organic matter to the pore water within the uppermost 8 cm (Fig. 2). Oxygen respiration, denitrification, manganese and iron reduction all may contribute to the phosphate release from organic substances. Almost constant dissolved total sulphur concentrations may indicate that sulphate reduction can be neglected at all three sites.

To estimate the single portions as well as the total rates, geochemical transport and reaction models have been used successfully (e.g. Slomp et al., 1996; Hensen et al., 1997). By comparison of the specific diffusive flux rates at site GeoB 9519 only (cf. Table 6) our data indicates that the P release from organic matter may occur predominantly via the oxic pathway (85%), followed by denitrification (14%). According to the simple calculation, the contribution of iron and manganese reduction together is only 1%. This small value corresponds perfectly to the slight increase of ammonium concentrations just at depth of iron reduction (Fig. 2). As mentioned before, release rates of P_{org} depend on the C:P ratio of the organic substrate decomposed. Assuming a constant C_{org}:P_{org} ratio of 350 (Fig. 6), in total 1.39 mmol P_{org} m^{-2} yr^{-1} would be released within the uppermost sediment layers at site GeoB 9519. The estimate connected with the modelled respiration of oxygen alone (1.2 mmol P_{org} m^{-2} yr^{-1}) is in very good correspondence with similar previous studies (e.g. Slomp et al., 1996). However, indicated by the virtually absence of phosphate concentration peaks, or at least significant changes in gradients within the uppermost 3 cm (Fig. 2), pore water data give also clear evidence that P_{org} can only be of relatively minor importance for the total dissolved phosphate pool at sites GeoB 9518 and 9519. Obviously, the major P release is closely associated with the reduction of iron (oxyhydr)oxides (cf. e.g. Krom and Berner, 1981; Sundby et al., 1992; Jensen et al., 1995; Slomp et al., 1998). Even with conservative calculations of about 4.5 and 3.5 mmol P m^{-2} yr^{-1}, respectively, release rates are much higher than estimates for the contribution of P_{org} to pore water phosphate (Table 6).

Beside the diffusive exchange across the sediment water interface, phosphate is removed from interstitial waters by association to iron (oxyhydr)oxides. The latter is reflected by the great similarity of phosphate and ferrous iron concentration profiles (Fig. 2; e.g. Krom and Berner, 1980; Lijklema, 1980). Fe minerals are characterized by a high surface area (e.g. Slomp et al., 1996) and high reactivity (e.g. Feely et al., 1990; Poulton and Canfield, 2006). Below the iron reduction zone, iron is probably fixed by the formation of iron sulfides. As depicted in Fig. 7a, total sulfur concentrations increase more than double within the lowermost 10 cm of all cores, from about 0.2 wt% within the oxic zone to more than 0.4 wt% at 18 cm sediment depth. However, the general increase of the total iron concentration with sediment depth in this area (Fig. 5) has recently been attributed to temporal decrease in the primary terrigenous input to these sediments during the last few thousand years (Mulitza et al., 2008).

Our data clearly indicate phosphate removal from the pore water below the iron reduction zone, potentially by the authigenic formation of P-minerals such as apatite, vivianite or calcite-associated (Figs. 3 and 7b; e.g. Burns, 1997; Hammond et al., 1999; Fagel et al., 2005; März et al., 2008). A discussion on such formation is not warranted by our data and is in any case beyond the scope of this paper.

4.2 Examination of the benthic budgets

A major question for the interpretation of geochemical data usually is, if the studied system was in a steady state at the time of sampling. This is of particular interest when specific transfer rates are calculated (or measured) to estimate their importance on time periods of hundreds or thousands of years. For marine sediments, this general question can be reworded into: Is there a balance between the transfer/transport processes as indicated by pore water concentration profiles (or direct rate measurements) and the composition of the sediment?

There are no indications for our study sites that major causes for non-steady state conditions have occurred. There is no active venting, there is no significant movement of redox boundaries relative to the sediment surface, and temporal changes in the bottom water oxygen concentration are unlikely. As a very probable approximation we will assume that steady state occurred, at least on moderate time scales. The lack of a clear decreasing %Corg versus sediment depth, and our radio carbon data suggest significant bioturbative benthic activity (cf. Fig. 6; Table 5). Comparing extraction- and porewater results, a few remarkable observations can be made: While the Fe:P ratios of the CDB-extractable mineral fraction (step 2) show values in a range already described in deep-sea sediments (24.4 to 32.0, Fig. 5 and 7c; Anschutz et al., 1998; Van der Zee et al., 2005), the distributions of solvents at site GeoB 9518 and GeoB 9519 indicate that the release of ferrous iron is only 2.9 to 4.0 times higher, respectively, than for phosphate (Table 6). Base on the stoichiometric range for the microbially catalyzed reduction of iron (oxyhydr)oxides, the degradation of organic matter cannot be a significant additional source for pore water phosphate (0.3–0.7% of the total phosphate release; Table 6). Even if the iron oxides, newly formed in the oxic zone, are very fine grained, poorly crystalline, and easily reducible, it seems very unlikely that such extremely low values reflect the ratios of the reduced mineral phase. This would be in contradiction to all reported knowledge on specific surface areas and adsorption capacities for iron oxides (Borggard, 1983; Crosby et al., 1983). However, there is clear evidence for low Fe(II):PO_4^{2-} release ratios at the depth of iron reduction (Fig. 2). A possible explanation could be a limited “etching” of mineral surfaces with their high phosphate covering density before the real crystal lattice is affected. Assuming steady state conditions, simple budget calculations reveal that the pore water system cannot be balanced by diffusive transport and sediment accumulation alone. Certainly, local enrichments, decreases or even total depletions in specific sediment fractions correspond to appropriate sinks and sources as indicated by the distribution of dissolved components. But the available amounts of mineral phases are by far not sufficient to maintain the diffusive flux or rather transfer rates for longer times. The downward decreases in Fe_{CDB} of 1.4 to 2.1 g kg^{-1} within an about 2 cm thick layer, are clearly caused by the reductive dissolution of iron (oxyhyxdr)oxides. Only by conservative burial due to simple accumulation onto sea floor, particles would pass this depth interval within a period of about 220–330 years, depending on the local sedimentation rate (Table 5). At sites GeoB 9518 and GeoB 9519, release rates of Fe^{2+}, constant for these periods, would require a demand of 6.7 and 5.6 mg cm^{-3} reducible iron oxides, respectively. These numbers are about 8 to 11 times higher than the detected decreases in Fe_{CDB}. Appropriate calculations for the re-oxidation of ferrous iron within the surface layer above iron reduction zone lead to similar results (Table 7). Possibly, the total amount of sedimentary iron oxides has not been extracted completely with CDB (Van der Zee et al., 2005), but even this cannot explain the detected differences.

The apparent discrepancy gets clearly visible when modelling the pore water concentration profiles by fitting the underlying transfer rates. The distribution of ferrous iron and iron mineral phases at site GeoB 9519 clearly illustrates this (Fig. 8). Negative values for transfer rates imply the release of iron (due to reductive dissolution), and positive values are equal to the fixation of dissolved iron (above: due to re-oxidation, below: probably due to the formation of iron sulphides). If molecular diffusion and sediment accumulation would be the only controlling factors for the benthic iron (and phosphate) cycle, both, the surface near enrichment of (oxyhydr)oxides and the depletion of iron within the iron reduction zone have had to be much more pronounced under the assumption of steady-state conditions. However, total iron concentrations are comparatively constant from 3 to 6 cm depth in GeoB 9519. Slight increases below 6 cm can be rather assigned to temporal changes in the terrigenous input than to effects of early diagenesis. However, obviously an additional transport process is necessary to explain our P_{CDB} and Fe_{CDB} data (Fig. 5). This additional process can only be a net downward transport of P-associated to iron (oxyhydr)oxides. Such an active internal replacement and cycling of particulate matter is caused by bioturbation, at least occasionally (e.g. Boudreau and Jørgensen, 2001 and refs. therein). Supported by results of one-dimensional reaction-transport modelling, Slomp et al. (1998) have already argued in a similar way the effects of bioturbation. The close correspondence between observed depth integrated iron content (Figs. 5 and 8) and its distribution deduced from transfer rates (Fig. 8), gives additional support to our interpretation. Anyway, if release and precipitation rates occur in the range as indicated by pore water data and if these rates seem constant over time, physical sediment mixing is an essential process to maintain a steady-state situation in the observed system.

5 Conclusions

Controlling processes for the benthic P- and Fe-cycles in marine surface sediments were investigated by means of pore water and solid phase analysis, balancing of release and precipitation rates, and the approach of a simple one-dimensional transport-reaction model. Biogenic-, Fe-, and organic-bound fractions are identified as the most important P-pools in these sediments. Calculations of transfer rates reveal that most of the dissolved phosphate is recently released to interstitial waters during the reduction of iron (oxyhydr)oxides. Comparing between release and precipitation rates, however, an apparent discrepancy is observed in the distribution of both sedimentary constituents. This balance approach clearly indicates the importance of particle mixing (bioturbation) for the maintenance of such system.

Acknowledgements. We want to thank the captain and crew of FS Meteor for their support during cruise M65/1. We highly appreciate the technical help onboard by C. März, S. Wiesmaier and S. Pape. We further want to thank B. Kockisch for TOC measurements and S. Pape, S. Siemer, N. Allroggen for sample preparation and lab assistance. This study was financed by the DFG International Graduate College EUROPROX.

References

Anderson, L. D., Delaney, M. L., and Faul, K. L.: Carbon to phosphorus ratios in sediments: Implications for nutrient cycling, Glob. Biogeochem. Cy., 15, 65–79, 2001.

Anderson, L. G., Turner, D. R., Wedburg, M., and Dyrssen, D.: Determination of total alkalinity and total dissolved inorganic carbon, in: Methods of Seawater Analysis, 3rd edition, edited by: Grasshoff, K., Kremling, K., Ehrhardt, M., Wiley-VCH, Weinheim, 127–148, 1999.

Anschutz, P., Zhong, S., Sundby, B., Mucci, A., and Gobeil, C.: Burial efficiency of phosphorus and the geochemistry of iron in continental margin sediments, Limnol. Oceanogr., 43, 53–64, 1998.

Barusseau, J. P., Giresse, P., Faure, H., Lezine, A. M., and Masse, J. P.: Marine sedimentary environments on some parts of the tropical and equatorial Atlantic margins of Africa during Late Quaternary, Cont. Shelf Res., 8, 1–21, 1988.

Baturin, G. N.: Phosphorites on the sea floor; Origin, composition and distribution, Elsevier, Amsterdam, 343 pp., 1982.

Borggard, O. K.: Effect of surface area and mineralogy of iron oxides on their surface charge and anion-adsorption properties, Clay Clay Miner., 31, 230–232, 1983.

Boudreau, B. P. and Jørgensen, B. B.: The benthic boundary layer: transport processes and biogeochemsitry, Oxfort University Press, US, 404 pp., 2001.

Burns, S. J.: Early diagenesis in Amazon Fan sediments, in: Proc. ODP Sci. Results, edited by: Flood, R. D., Piper, D. J. W., Klaus, A., and Peterson, L. C., College Station, Texas, 497–504, 1997.

Crosby, S. A., Glasson, D. R., Cuttler, A. H., Butler, I., Turner, D. R., Whitfield, M., and Millward, G. E.: Surface areas and porosities of Fe(III)-Fe(II)-derived oxyhydroxides, Environ. Sci. Technol., 17, 709–713, 1983.

De Lange, G. J., Cranston, R. E., Hydes, D. H., and Boust D.: Extraction of pore water from marine sediments: A review of possible artifacts with pertinent examples from the North Atlantic, Mar. Geol., 109, 53–76, 1992.

De Lange, G. J.: Distribution of various extracted phosphorus compounds in the interbedded turbiditic/pelagic sediments of the Madeira Abyssal Plain, eastern North Atlantic, Mar. Geol., 109, 115–139, 1992.

Dickens, G. R., Koelling, M., Smith, D. C., Schnieders, L., and Scientists: Rhizon Sampling of Pore Waters on Scientific Drilling Expeditions: An Example from the IODP Expedition 302, artic coring expedition (ACEX), Scientific Drilling, 4, 22–25, 2007.

Fagel, N., Alleman, L. Y., Granina, L., Hatert, F., Thamo-Boszo, E., Cloots, R., and André, L.: Vivianite formation and distribution in Lake Baikal sediments, Global Planet. Change, 46, 315–336, 2005.

Feely, R. A., Massoth, G. J., Baker, E. T., Cowen, J. P., Lamb, M. F., and Krogslund, K. A.: The effect of hydrothermal processes on midwater phosphorus distributions in the northeast Pacific, Earth Planet. Sc. Lett., 96, 305–318, 1990.

Föllmi, K. B.: The phosphorus cycle, phosphogenesis and marine phosphate-rich deposits, Earth-Sci. Rev., 40, 55–124, 1996.

Froelich, P. N., Klinkhammer, G. P., Bender, M. L., Luedtke, N. A., Heath, G. R., Cullen, D., Dauphin, P., Hammond, D., Hartman, B., and Maynard, V.: Early oxidation of organic matter in pelagic sediments of the eastern equatorial Atlantic: suboxic diagenesis, Geochim. Cosmochim. Ac., 43, 1075–1090, 1979.

Froelich, P. N., Arthur, M. A., Burnett, W. C., Deakin, M., Hensley, V., Jahnke, R., Kaul, L., Kim, K.-H., Roe, K., Soutar, A., and Vathakanon, C.: Early diagenesis of organic matter in Peru continental margin sediments: Phosphorite precipitation, Mar. Geol., 80, 309–343, 1988.

Hagen, E.: Mesoscale upwelling variations off the West African coast, in: Coastal and Estuarine Sciences, Coastal Upwelling, 1st edition, edited by: Richards, F. A., AGU, Washington DC, 72–78, 1981.

Hagen, E.: Northwest African upwelling scenario, Oceanol. Acta, 24, 113–128, 2000.

Hall, P. O. J. and Aller, R. C.: Rapid, small-volume, flow injection analysis for δCO_2, and NH_4^+ in marine and freshwaters, Limnol. Oceanogr., 37, 1113–1119, 1992.

Hammond, D. E., Giordani, P., Berelson, W. M., and Poletti, R.: Diagenesis of carbon and nutrients and benthic exchange in sediments of the Northern Adriatic Sea, Mar. Chem., 66, 53–97, 1999.

Hansen, H. P. and Koroleff, F.: Determination of nutrients, in: Methods in seawater analysis, 3rd Ed., edited by: Grasshoff, K., Ehrhardt, M., Kremling, K., Wiley-VCH, Weinheim, 159–228, 1999.

Hartmann, M. P., Müller, P. J., Suess, E., and Van der Weijden, C. H.: Chemistry of Late Quaternary sediments and their interstitial waters from the NW African continental margin, Meteor Forschungsergebnisse Ser. C, Hamburg, 24, 1–67, 1976.

Helmke, P., Romero, O., and Fischer, G.: Northwest African upwelling and its effect on offshore organic carbon export to the deep sea, Glob. Biogeochem. Cy., 19, 1–15, doi:10.1029/2004GB002265, 2005.

Hensen, C., Landenberger, H., Zabel, M., Gundersen, J. K., Glud, R. N., and Schulz, H. D.: Simulation of early diagenetic processes in continental slope sediments off southwest Africa: the computer model CoTAM tested, Mar. Geol., 144, 191–210, 1997.

Hensen, C., Landenberger, H., Zabel, M., and Schulz, H. D.: Qualification of diffusive benthic fluxes of nitrate, phosphate and silicate in the South Atlantic Ocean, Glob. Biogeochem. Cy., 12, 277–300, 1998.

Ingall, E. D. and Van Cappellen, P.: Relation between sedimentation rate and burial of organic phosphorus and organic carbon in marine sediments, Geochim. Cosmochim. Ac., 54, 373–386, 1990.

Ingall, E. D. and Jahnke, R.: Evidence for enhanced phosphorus regeneration from marine sediments overlain by oxygen depleted waters, Geochim. Cosmochim. Ac., 58, 2571–2575, 1994.

Inthorn, M., Wagner, T., Scheeder, G., and Zabel, M.: Lateral transport controls distribution, quality, and burial of organic matter along continental slopes in high-productivity areas, Geology, 34, 205–208, 2006.

Jahnke, R. A., Emerson, S. R., Reimers, C. E., Schuffert, J., Ruttenberg, K. C., and Archer, D.: Benthic recycling of biogenic debris in eastern equatorial Atlantic Ocean, Geochim. Cosmochim. Ac., 53, 2947–2960, 1989.

Jensen, H. S., Mortensen, P. B., Andersen, F. O., Rasmussen, E., and Jensen, A.: Phosphorus cycling in a coastal marine sediment, Aarhus Bay, Denmark, Limnol. Oceanogr., 40, 908–917, 1995.

Kim, D., Schuffert, J. D., and Kastner, M.: Francolite authigenesis in california continental slope sediments and its implications for the marine P cycle, Geochim. Cosmochim. Ac., 63, 3477–3485, 1999.

Koroleff, F. and Kremling, K.: Determination of trace elements – Analysis by spectrophotometry, in: Methods of Seawater Analysis, 3rd Ed., edited by: Grasshoff, K., Kremling, K., Ehrhardt, M., Wiley-VCH, Weinheim, 340–344, 1999.

Krom, M. D. and Berner, R. A.: Adsorption of phosphate in anoxic marine sediments, Limnol. Oceanogr., 25, 797–806, 1980.

Krom, M. D. and Berner, R. A.: The diagenesis of phosphorus in a nearshore sediment, Geochim. Cosmochim. Ac., 45, 207–216, 1981.

Latimer, J. C., Filippelli, G. M., Hendy, I., and Newkirk, D. R.: Opal-associated particulate phosphorus: Implications for the marine P cycle, Geochim. Cosmochim. Ac., 70, 3843–3854, 2006.

Lijklema, L.: Interaction of orthophosphate with iron(III) and aluminum hydroxides, Environ. Sci. Technol., 14, 537–541, 1980.

Lutze, G. F. and Coulbourn, W. T.: Recent benthic foraminifera from the continental margin of northwest Africa: Community structure and distribution, Mar. Micropaleontol., 8, 361–401, 1984.

März, C., Hoffmann, J., Bleil, U., De Lange, G. J., and Kasten, S.: Diagenetic changes of magnetic and geochemical signals by anaerobic methan oxidation in sediments of the Zambesi deep-sea fan (SW Indian Ocean), Mar. Geol., 255, 118–130, 2008.

McMaster, R. L. and Lachance, T. P.: Northwestern African continental shelf sediments, Mar. Geol., 7, 57–67, 1969.

Mittelstaedt, E.: The upwelling area off Northwest Africa – A description of phenomena related to coastal upwelling, Prog. Oceanogr., 12, 307–331, 1983.

Mollenhauer, G., Inthorn, M., Vogt, T., Zabel, M., Sinninghe Damste, J. S., and Eglinton, T. I.: Aging of marine organic matter during cross-shelf lateral transport in the Benguela upwelling system revealed by compound-specific radiocarbon dating, G3, 8, Q09004, doi:09010.01029/02007GC001603, 2007.

Mulitza, S., Bouimetarhan, I., Brüning, M., Freesemann, A., Gussone, N., Filipsson, H., Heil, G., Pape, S., Jaeschke, A., Johnstone, H., Klann, M., Klein, F., Küster, K., März, C., McGregor, H., Minning, M., Müller, H., Ochsenhirt, W.-T., Paul, A., Schewe, F., Schulz, M., Steinlöchner, J., Stuut, J.-B., Tjallingii, T., v. Dobeneck, T., Wiesmeier, S., Zabel, M., and Zonneveld, K. A. F.: Report and preliminary results of Meteor cruise M65/1, Dakar – Dakar, 11.06.–1.07.2005, Berichte FB Geowissenschaften University of Bremen, 252, 149 pp., 2006.

Mulitza, S., Prange, M., Stuut, J.-B., Zabel, M., Dobeneck, T. v., Intambi, C., Nizou, J., and Schulz, M.: Sahel megadroughts triggered by glacial slowdowns of Atlantic meridional overturning, Paleoceanography, 23, doi:10.1029/2008PA001637, 2008.

Nadeau, M. J., Schleicher, M., Grootes, P. M., Erlenkeuser, H., Gottdang, A., Mous, D. J. W., Sarnthein, J. M., and Willkomm, H.: The Leibniz-Labor AMS facility at the Christian-Albrechts University, Kiel, Germany, Nucl. Instrum. Methods Phys. Res. Sec. B, 123, 22–30, 1997.

Poulton, S. W. and Canfield, D. E.: Co-diagenesis of iron and phosphorus in hydrothermal sediments from the southern East Pacific Rise: Implications for the evaluation of paleoseawater phosphate concentrations, Geochim. Cosmochim. Ac., 70, 5883–5898, 2006.

Redfield, A. C., Ketchum, B. H., and Richards, F. A.: The influence of organisms in the composition of sea-water, in: The composition of seawater. Comparative and descriptive oceanography. The Sea: ideas and observations on progress in the study of the seas, 1st edition, edited by: Hill, M. N., Interscience, New York, 26–77, 1963.

Ruttenberg, K. C.: Development of a sequential extraction method for different forms of phosphorus in marine sediments, Limnol. Oceanogr., 37, 1460–1482, 1992.

Schenau, S. J. and De Lange, G. J.: A novel chemical method to quantify fish debris in marine sediments, Limnol. Oceanogr., 45, 963–971, 2000.

Schenau, S. J., Slomp, C. P., and De Lange, G. J.: Phosphogenesis and active phosphorite formation in sediments from the Arabian Sea oxygen minimum zone, Mar. Geol., 169, 1–20, 2000.

Schulz, H. D., Dahmke, A., Schinzel, U., Wallmann, K., and Zabel, M.: Early diagenetic processes, fluxes, and reaction rates in sediments of the South Atlantic, Geochim. Cosmochim. Ac., 58, 2041–2060, 1994.

Schulz, H. D. and Schulz, H. N.: Large Sulfur Bacteria and the Formation of Phosphorite, Science, 307, 416–418, 2005.

Schulz, H. D.: Quantification of Early Diagenesis: Dissolved Constituents in Pore Water and Signals in the Solid phase, in: Marine Geochemistry, 2nd Ed., edited by: Schulz, H. D. and Zabel, M., Springer-Verlag, Berlin, Heidelberg, New York, 75–124, 2006.

Seeberg-Elverfeldt, J., Schlüter, M., Feseker, T., and Kölling, M.: Rhizon sampling of porewaters near the sediment-water interface in aquatic systems, Limn. Oceanogr-Meth., 3, 361–371, 2005.

Slomp, C. P., Epping, E. H. G., Helder, W., and Van Raaphorst, W.: A key role for iron-bound phosphorus in authigenc apatite formation in North Atlantic continental platform sediments, J. Mar. Res., 54, 1179–1205, 1996.

Slomp, C. P., Malschaert, J. F. P., and Van Raaphorst, W.: The role of adsorption in sediment-water exchange of phosphate in North Sea continental margin sediments, Limnol. Oceanogr., 43, 832–846, 1998.

Strickland, J. D. H. and Parsons, T. R.: A practical handbook of seawater analysis, Fisheries Research Board of Cananda, Ottawa, 293 pp., 1968.

Summerhayes, C. P.: Sedimentation of organic matter in upwelling regimes, in: Coastal upwelling – Its Sediments Record Part B: Sedimentary records of ancient coastal upwelling, 1st Ed., edited by: Suess, E. and Thiede, J., Plenum Press, New York, 29–72, 1983.

Sundby, B., Gobeil, C., Silverberg, N., and Mucci, A.: The phosphorus cycle in coastal marine sediments, Limnol. Oceanogr., 37, 1129–1145, 1992.

Takahashi, T., Broecker, W. S., and Langer, S.: Redfield Ratio based on chemical data from isopycnal surfaces, J. Geophys. Res., 90, 6907–6924, 1985.

Van Cappellen, P. and Ingall, E. D.: Benthic phophorus regeneration, net primary production, and ocean anoxia: A model of the coupled marine biogeochemical cycles of carbon and phosphorus, Paleoceanography, 9, 677–692, 1994.

Van der Zee, C., Slomp, C. P., Rancourt, D. G., De Lange, G. J., and Van Raaphorst, W.: A Mössbauer spectroscopic study of the iron redox transition in eastern Mediterranean sediments, Geochim. Cosmochim. Ac., 69, 441–453, 2005.

Zabel, M., Dahmke, A., and Schulz, H. D.: Regional distribution of diffusive phosphate and silicate fluxes through the sediment-water interface: the eastern South Atlantic, Deep-Sea Res. I, 45, 277–300, 1998.

Zabel, M., Bickert, T., Dittert, L., and Haese, R. R.: The significance of the sedimentary Al/Ti ratio as indicator for reconstructions of terrestrial input to the equatorial Atlantic, Paleoceanography, 14, 789–799, 1999.

Zabel, M. and Schulz, H. D.: Importance of submarine landslides for non-steady state conditions in pore water systems – lower Zaire (Congo) deep-sea fan, Mar. Geol., 176, 87–99, 2001.

Table 1. Location and water depth (m), surface total organic carbon (TOC) and $CaCO_3$ content (wt%).

GeoB site	Latitude	Longitude	Water depth (m)	TOC (wt%)	$CaCO_3$ (wt%)
9510-3	15°25.0′ N	17°39.2′ W	1567	2.4	13.5
9519-6	13°48.7′ N	17°40.9′ W	1488	2.9	10.5
9518-4	13°47.6′ N	17°47.4′ W	1997	2.8	8.1

Table 2. Summary of pore water analysis, methods and references.

Analysis	Method	Reference
Alkalinity	Titration	Anderson et al., 1999
Ammonium	Conductivity	Hall and Aller, 1992
Ferrous iron	Photometrically	Koroleff and Kremling, 1999
Manganese, sulphur	ICP-OES	Perkin Elmer, Optima 3000
Nitrate	Photometrically	Hansen and Koroleff, 1999
Phosphate	Photometrically	Strickland and Parsons, 1972; Hansen and Koroleff, 1999

Table 3. Sequential extraction steps (after Ruttenberg, 1992; Schenau and De Lange, 2000; Latimer et al., 2006).

Step	Reagents	P component extracted
(1) Biogenic	25 mL 2M NH_4Cl (pH 7)	remaining pore water P, exchangeable P, biogenic apatite, apatite precursor mineral, $CaCO_3$-bound P
(2) Oxide-associated	25 mL citrate dithionite buffer (pH 7.5), 25 mL 2 M NH_4Cl, 25 mL dem. water	adsorbed and reducable/ reactive Fe-bound P
(3) Authigenic	25 mL 1 M Na-acetate (pH 4), 25 mL 2 M NH_4Cl, 25 mL dem. water	authigenic P
(4) Detrital	25 mL 1 M HCl, 25 mL dem. water	detrital P
(5) Organic	after ignition at 550°C 25 mL 1 M HCl	organic P
(6) Opal	25 mL 1.5 M NaOH at 85°C	opal-associated P

Table 4. Mean P concentration (g P kg^{-1}) and *percentages* %.

GeoB site	Biogenic P	Oxide P	Authigenic P	Detrital P	Organic P	Opal P
9510	0.17 *(24)*	0.21 *(29)*	0.05 *(7)*	0.08 *(11)*	0.21 *(29)*	–
9519	0.25 *(32)*	0.20 *(26)*	0.04 *(3)*	0.09 *(11)*	0.20 *(26)*	–
9518	0.15 *(23)*	0.22 *(33)*	0.03 *(4)*	0.03 *(5)*	0.17 *(24)*	0.07 *(11)*

Table 5. MS ^{14}C-ages (yrs BP) and corresponding sedimentation rates (SR) (cm kyr^{-1}).

Sediment depth (cm)	GeoB 9510	GeoB 9519	GeoB 9518
0–0.5	719	1113	800
4–5	1581	–	1345
7.5–10	1175	2602	2549
15–20	3200	2660	2290
SR	6.2	8.6	7.3

Table 6. Release rates of phosphate (P) and iron (Fe) as calculated from diffusive fluxes (mmol m^{-2} yr^{-1}); C_{org}:P_{org}=350^a or 106^b; * calculation impossible on account of artificial data.

Benthic nutrient fluxes	GeoB 9510	GeoB 9518	GeoB 9519
Release of P during oxic degradation of organic matter	n.d.*	1.7^a–5.7^b	1.2^a–3.8^b
Release of P during denitrification	0.23^a–0.77^b	0.20^a–0.65^b	0.19^a–0.62^b
Total release of P during reductive dissolution of Fe-(oxyhydr)oxides	n.d.*	4.50	3.54
Release of P from organic matter during iron reduction	n.d.*	0.012^a–0.031^b	0.010^a–0.033^b
Release of Fe during reductive dissolution of Fe-(oxyhydr)oxides	n.d.*	12.95	14.03

Table 7. Simplified budget of transfer rates connected with the reduction of iron (oxyhydr)oxides assuming steady state Fe^{2+} release/precipitation rates;with wet bulk density: 0.4 (g cm^{-3}); *calculation impossible on account of artificial data.

Parameter	Unit	GeoB 9510	GeoB 9518	GeoB 9519
~SR	cm kyr^{-1}	6	7	9
Age of a 2 cm interval (Δt)	yrs	333	286	222
Fe_{CDB} decrease within this interval at depth of iron reduction (Fig. 7c)	g kg^{-1} Δt^{-1} mg cm^{-3} Δt^{-1}	2.1 0.8	1.4 0.6	1.8 0.7
Fe^{2+} release (cf. Table 6)	mg cm^{-3} Δt^{-1}	n.d.*	6.7	5.6
Fe^{2+} re-oxidation	mg cm^{-3} Δt^{-1}	n.d.*	5.0	4.0
Fe_{CDB} max.-surface	g kg^{-1} Δt^{-1}	0.9	0.4	0.7

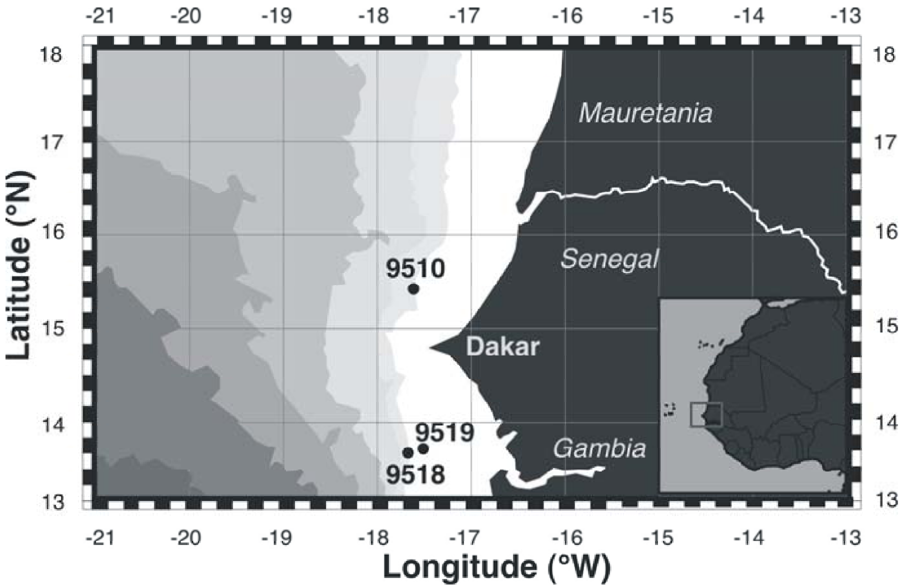

Fig. 1. Sampling locations along the NW-African continental margin.

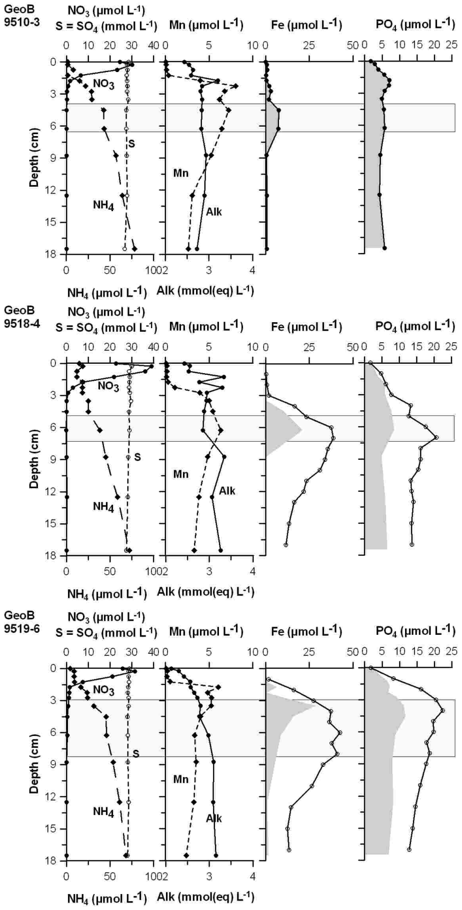

Fig. 2. Depth profiles of dissolved nitrate, ammonium and sulphur, manganese, alkalinity (mmol(eq) L^{-1}), ferrous iron and phosphate in pore water (µmol L^{-1}). Grey bars mark the area of reductive dissolution of iron (oxyhydr)oxides. Dashed lines represent pore water concentrations of ferrous iron and phosphate measured in rhizon samples, shaded area the concentrations measured in squezzer samples.

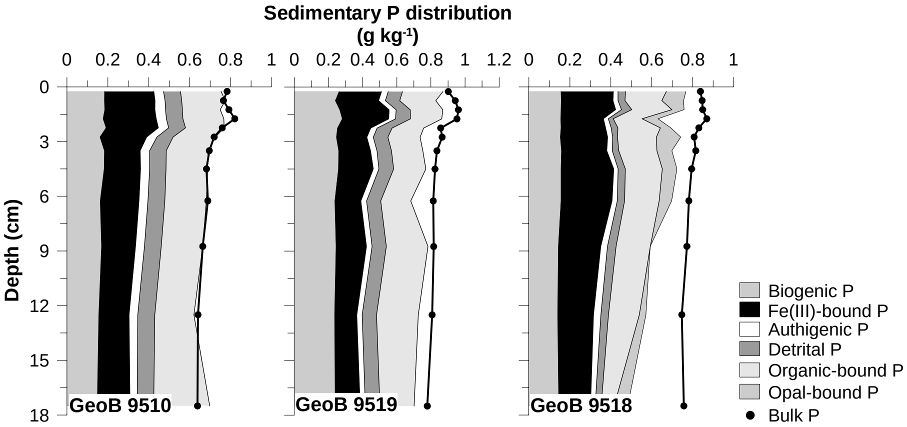

Fig. 3. Sedimentary P distribution (g kg^{-1} dry sediment).

Title Page
Abstract
Introduction
Conclusions
References
Tables
Figures
◄◄
►►
◄
►
Back
Close
Full Screen / Esc
Printer-friendly Version
Interactive Discussion

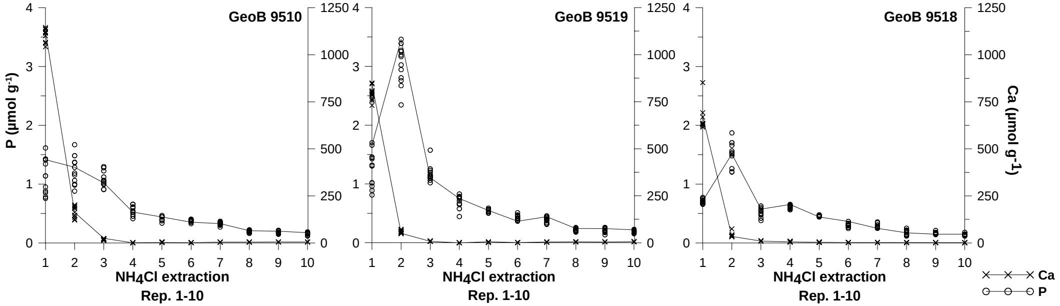

Fig. 4. Sequential extraction of calcium and phosphorus with NH_4Cl ($\mu mol\,g^{-1}$ dry sediment), multiple analyses of each sample; single dotes are the measured P values, single crosses the measured Ca values, solid lines represent the average values of each single extraction step.

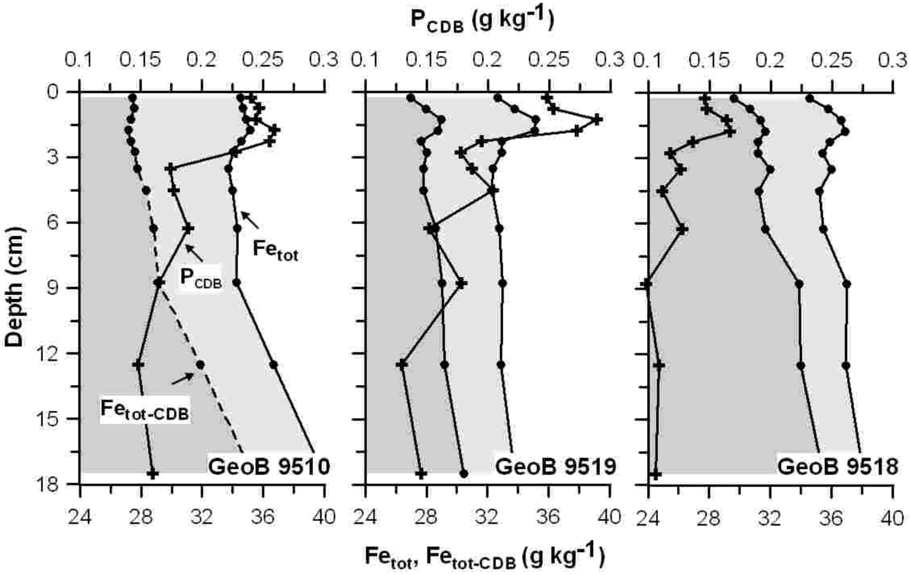

Fig. 5. CDB extractable P and bulk Fe content, and bulk Fe reduced by the content of iron (oxyhydr)oxides (Fe_{CDB}) in g kg^{-1} dry sediment.

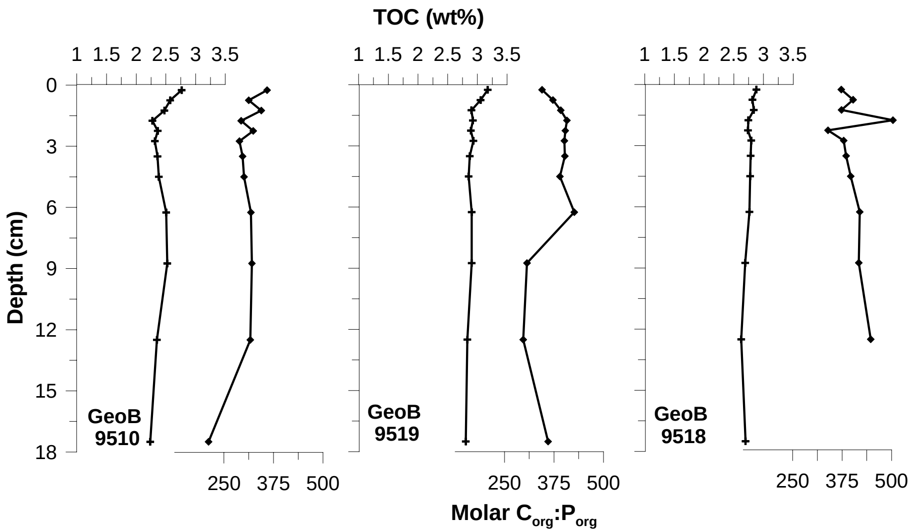

Fig. 6. Depth profiles of total organic carbon content (wt%), and molar C_{org}:P_{org} ratios.

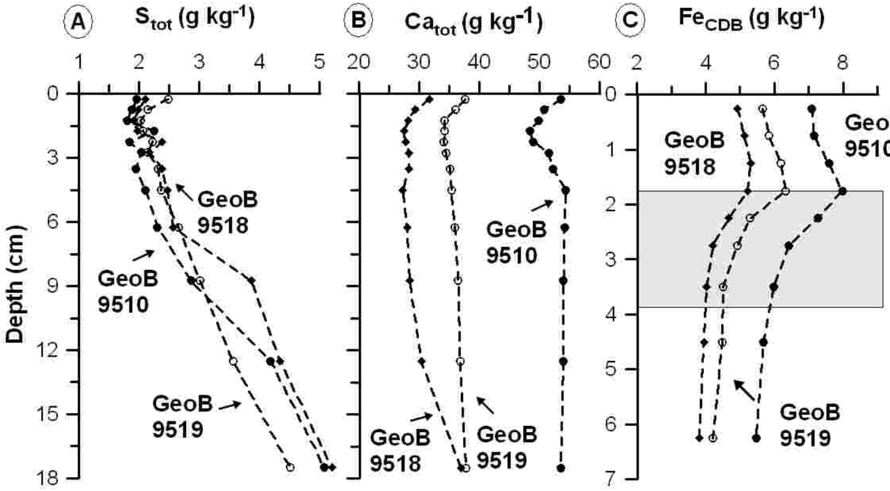

Fig. 7. **(A)** bulk S, **(B)** bulk Ca, and **(C)** CDB extractable Fe content (g kg^{-1} dry sediment).

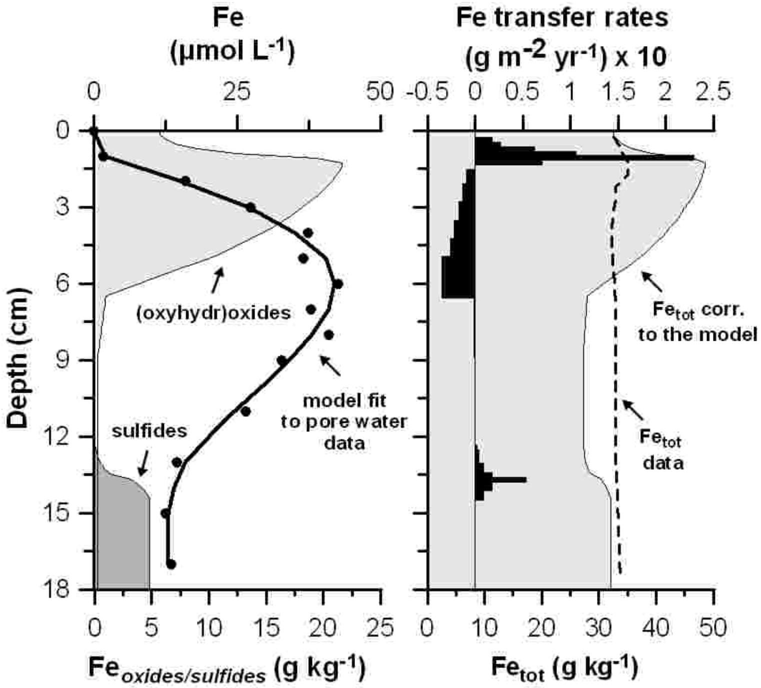

Fig. 8. Left: model fit to ferrous iron profile at site GeoB 9519 in comparison to the distribution of particulate iron mineral phases ($Fe_{oxides/sulfides}$). Right: distribution of iron mineral phases (Fe_{tot}, Fe_{tot} corrected to model fit) and transfer rates (negative values: release due to reductive dissolution; positive values: fixation of dissolved iron).